J. Schroeder, D. Schwarzer, J. Troe, and F. Voß

Cluster and barrier effects in the temperature and pressure dependence of the photoisomerization of *trans*-stilbene

J. Schroeder, D. Schwarzer, J. Troe, and F. Voβ

Institut für Physikalische Chemie der Universität Göttingen, Tammannstr. 6, D-3400 Göttingen, West Germany

The pressure and temperature dependence of the photoisomerization rate coefficient of *trans*-stilbene in the S_1 state have been measured in the solvents C_2H_6, C_3H_8, C_4H_{10}, Xe, Co_2, SF_6, and CHF_3. At constant temperature, the pressure dependences up to 6 kbar can be well represented by the Kramers–Smoluchowski model. The comparison of results in different solvents clearly indicates the importance of reactant–solvent cluster formation modifying the height and imaginary frequency of the barrier. The change of the temperature dependence with pressure points towards a multidimensional barrier of nonseparable character. Multidimensional barrier effects manifest themselves most clearly via the temperature dependence of the rate coefficient in the Kramers–Smoluchowski limit.

I. INTRODUCTION

The dynamics of reactions in liquids is strongly influenced by interactions of the reactants with the surrounding solvent medium. Energy transfer between reactant and solvent molecules, transport processes, and reactant—solvent interactions modifying the potential energy surface of the reaction, play an important role. In general, these different aspects of the reaction dynamics in solution are difficult to separate experimentally. We have recently shown, however, that the individual contributions of the interaction influence barrier crossing processes in different ways in different density regimes.[1] By studying the pressure and temperature dependence of the S_1 photoisomerization of 1,4—diphenylbutadiene (DPB), from low densities in the gas phase to high densities in the compressed liquid phase, we were able to identify solvent-specific cluster effects in the low density regime and manifestations of the multidimensional character of the barrier crossing process in the high density region. We also could show that Kramers theory adequately describes the reaction rate in alkane solvents at viscosities up to 1 cP.

In the present work, we describe related experiments for the unimolecular isomerization of *trans*-stilbene in its first excited singlet state. This photochemical "model" reaction has been extensively studied under a large variety of experimental conditions (for work prior to 1980 see, e.g., Refs. 2 and 3). During the past decade, experiments on isolated stilbene molecules in supersonic jets[4-9] and low pressure gases,[10-15] time resolved studies of the solvent dependence of the reaction rate coefficient in various solvent series,[16-21] and the investigation of its temperature dependence in alkanes[22-28] and alcohols,[29] have greatly improved our detailed understanding of stilbene photoisomerization dynamics in solution. However, as we have discussed for the case of DPB,[1] there remain a number of open questions which we address again in the present article:

(*i*) *Cluster effects in the low friction regime.* RRKM modeling[30] of the energy-specific rate coefficients for *trans*-stilbene S_1 photoisomerization measured in supersonic jets[4,5] and low pressure vapor[10] led to a reaction threshold in the S_1 state of $E_0 = 15.6$ kJ/mol for isolated *trans*-stilbene and a prediction of the high pressure rate coefficient k_∞ of the thermal unimolecular reaction of the form $k_\infty = 8.3 \times 10^{11} \exp(-15.0 \text{ kJ mol}^{-1}/RT) \text{ s}^{-1}$. The predicted value, however, is more than one order of magnitude lower than the rate coefficient measured in low viscosity liquids[26,31] and in the gas phase at high pressure.[31-33] On the basis of our investigation of the pressure dependence of the rate coefficient in ethane and propane solvent, we have proposed that this discrepancy can be understood in terms of a "solvent shift" of the reaction barrier due to complex formation between *trans*-stilbene and solvent molecules setting in at fairly low pressures in the gas phase.[31] In the photoisomerization of DPB the discrepancy between predicted and measured low viscosity rate coefficients is only small.[34] Nevertheless, there is evidence for cluster effects lowering the reaction barrier also in this case.[1,35] By employing different kinds of solvent molecules, we could show that this effect is solvent specific. The question arises whether such solvent specificity pertains for stilbene S_1 isomerization as well. For this purpose, we have extended preliminary low pressure experiments[36] in different supercritical solvents. They provide another test of the applicability of the solvent shift model[37] in view of alternative interpretations[27,38-40] and criticisms.[41]

(*ii*) *Kramers–Smoluchowski behavior in the high friction regime.* The dependence of the photoisomerization rate of *trans*-stilbene[19,25,42] and DPB[42,43] on friction in larger alkane solvents has been observed to deviate significantly from the inverse viscosity dependence expected in the high friction Kramers–Smoluchowski limit

$$k \propto k_\infty / \eta. \tag{1}$$

Instead, a relationship

$$k \propto k_\infty / \eta^a \quad \text{with } a < 1 \tag{2}$$

was found. These results were obtained by studying series of *n*-alkane solvents (larger than *n*-butane) mostly at ambient

pressure. A better test for the validity of the Kramers–Smoluchowski description of the reaction, however, is provided by the investigation of the pressure dependence in single solvents along different isotherms. We have employed this approach in a number of earlier studies.[37] Our recent work on the pressure dependence of the photoisomerization of DPB[1] confirmed the advantage of this method. Within a single solvent, for the small alkanes (C_2–C_4) using pressures up to 6.5 kbar, the viscosity dependence apparently was well described by Kramers theory. In the present article, extending our earlier studies,[31,35,36] the corresponding experiments on *trans*-stilbene are reported.

(*iii*) *Multidimensional barrier crossing.* The comparison of the temperature dependences of the DPB photoisomerization rate coefficient in different friction regimes suggested that the strong temperature effects at high friction represent a manifestation of the multidimensional character of the barrier crossing process.[1] Apparently, the reaction rate is very sensitive to the properties of the multidimensional potential energy surface in the barrier region, such that the reaction flow pattern strongly depends on the thermal excitation of the various low frequency modes "perpendicular to the reaction coordinate".

Multidimensional effects in barrier crossing problems have found attention in a number of recent publications. There is the "trivial" multidimensional behavior in the weak-damping region, where standard unimolecular rate theory applies.[37,44–46] For a while, this has been overlooked in discussions of one-dimensional "Kramers turnovers"; it is, however, generally accepted now.[47] Multidimensional effects in the strong-damping regime[48–51] may be due to anisotropic friction.[52,53] The topology of the barrier region also can play a role,[54–56] which may manifest itself in form of the temperature dependence of the rate coefficient.[1] Deviations from an inverted parabolic potential in the reaction coordinate also lead to deviations of the temperature dependence from that given by k_∞ in Eq. (1). However, the effects observed in Ref. 1 were far too large to be explained in this way. Instead, we attributed our results to a dependence of the imaginary barrier frequency in the reaction coordinate on the excitation of coordinates perpendicular to the reaction coordinate. The present work reports experimental results on the *trans*-stilbene system which may be interpreted in the same way. Our quantum-chemical calculations for stilbene[57] demonstrated the complicated character of the potential energy surface in the saddle point region which can be the reason for the suggested behavior.

II. EXPERIMENTAL TECHNIQUE

Rate coefficients for thermal isomerization of electronically excited *trans*-stilbene after excitation at 308 nm were determined from the transient absorption decay at 616 nm. The FWHM of the UV-excitation pulse was approximately 5 ps, its value for the red probe pulse was 2.5 ps. The pump pulse energy hitting the sample was about 0.3 mJ at 308 nm, and the energy of the 616 nm probe pulse was about 0.05 mJ. Pulse energies were measured in front of and behind the sample cell with photodiodes, whose output was integrated, digitized, and fed into a computer. The output of the pump–

pulse photodiode was monitored and used to reject measurements with more than 15% deviation from the average pump energy. The plane of polarization of the probe beam could be varied by means of a zero-order half-wave plate to eliminate the effects of overall rotational relaxation on the transient absorption signals. Samples of 200 nm thickness were used in high pressure gas phase experiments, and of 20 or 1.8 mm in liquid phase measurements. The temperature of the cell was controlled to one degree accuracy in gas phase experiments. The cell windows were kept at a slightly higher temperature than the cell body in order to avoid photocondensation on the inner surface of the sapphire windows. Solvents, gases, and *trans*-stilbene were of the highest commercially available purity and used without further purification. Further details of our experiments setup and technique were reported earlier.[1,31]

III. EXPERIMENTAL RESULTS

The transient absorption of *trans*-stilbene at 616 nm, which was measured in a "magic" angle arrangement[58] of the planes of polarization of pump and probe pulses, showed a rapid increase with a rise time of about 5 ps followed by a slower decay characterized by first-order kinetics with rate coefficients k_{expt}. The rise time corresponded to the cross-correlation width of pump and probe pulse and reflected the time resolution of the present experiments. The transient absorption was assigned to the lowest excited singlet state of *trans*-stilbene in solution.[16,18,59] Figure 1 shows an absorption–time profile and the corresponding blank signal obtained without pump pulse. We obtained the isomerization rate coefficient by subtracting the radiative rate coefficient[22] $k_r = 6 \times 10^8$ s^{-1} from the measured first-order decay rate coefficient. We assumed that the nonradiative decay of the observed excited singlet state of *trans*-stilbene is dominated by rotation about the double bond,[2,60] and the subsequent internal conversion to the electronic ground state is a much faster process.[61] The resulting rate coefficients
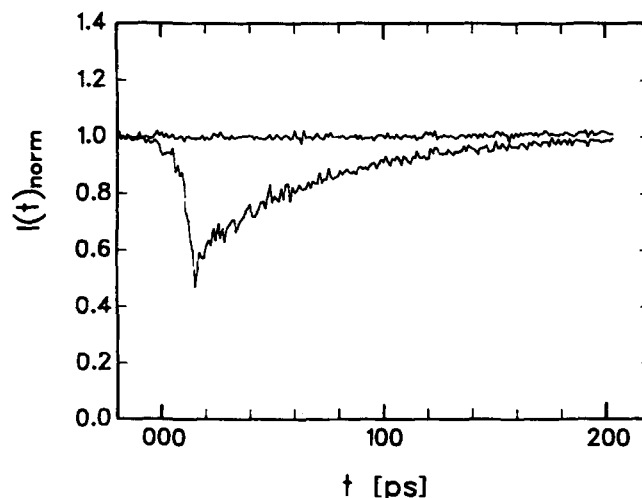

FIG. 1. Absorption–time profile of the photoisomerization of *trans*-stilbene in ethane ($p = 6.4$ MPa; $T = 295$ K). Plot of normalized transmitted intensity at 616 nm vs time. Upper trace: without UV excitation; lower trace: with excitation at 308 nm. Each trace consists of 250 discrete data points.

$k = k_{expt.} - k_r$ are listed in Tables I–IV for liquid and super-critical fluid solvents together with the corresponding solvent concentrations, viscosities, and self-diffusion coefficients. Diffusion coefficients for liquid and dense fluid solvents were taken directly or extrapolated from experimental self-diffusion coefficients or viscosity data (for references, see footnotes of Tables I–IV). For the low density gas phase, gas kinetic diffusion coefficients were calculated using pVT data and Lennard-Jones collision integrals.[62]

Figure 2 shows the rate coefficients k measured in eth-

ane, propane, and *n*-butane as a function of the inverse of the solvent self-diffusion coefficient D^{-1}. The k values decrease by about one order of magnitude when the pressure is raised from about 1 to 600 MPa in the liquid phase. In the compressed liquid, the rate coefficients approach proportionality to the self-diffusion coefficient in all three solvents. At constant diffusion coefficient, the limiting high viscosity values increase roughly by 70% from ethane to propane, and by 50% from propane to *n*-butane. The gas phase measurements had to be performed at a higher temperature to obtain a sufficient vapor pressure of stilbene. They were converted to the temperature of the liquid phase experiments using the

TABLE I. Rate coefficients k for photoisomerization of *trans*-stilbene in supercritical ethane.

p/MPa	T/K	$[M]/10^{-2}$ mol cm^{-3}	η/cP[a]	$D/10^{-4}$ cm^2 s^{-1}	$k/10^{10}$ s^{-1}
2.6	350	0.100[b]	0.012[b]	43.3[d]	6.8
2.7	366	0.108	0.012	42.3	6.0
2.8	311	0.221	0.010	37.8	5.0
6.5	368	0.291	0.015	15.6	8.0
8.6	433	0.294	0.018	17.9	10.3
10.0	422	0.366	0.019	14.1	9.0
15.1	413	0.625	0.024	8.1	8.9
12.0	330	1.075	0.039	3.8	3.8
20.0	330	1.25	0.052	3.6[e]	3.6
150	330	1.79[c]		1.4	2.4
180	330	1.84		1.3	2.0
240	330	2.00		0.96	1.7
300	330	2.05		0.84	1.5
370	330	2.12		0.65	1.4
430	330	2.16		0.60	1.3
5.9	356	0.282[b]	0.014	15.6[d]	6.0
8.7	356	0.535	0.019	8.2	5.6
16.6	356	1.06	0.038	4.2	5.4
20.0	356	1.11	0.044	3.9[e]	4.1
50.0	356	1.42	0.087	2.6	3.7
10.0	375	0.518	0.020	8.9[d]	8.0
19.2	375	0.974	0.037	4.8	7.5
124	375	1.73[c]		1.7[e]	5.8
140	375	1.80		1.6	5.1
8.2	306	1.18[b]	0.045	3.7[d]	2.8
8.6	309	1.14	0.042	3.6	2.8
9.5	313	1.12	0.043	3.7	2.8
10.4	318	1.12	0.042	3.7	3.3
11.0	322	1.11	0.041	3.7	3.5
7.5	325	0.815	0.026	5.0	4.0
13.5	335	1.07	0.041	3.9	5.1
14.0	338	1.05	0.040	4.0	4.9
10.6	343	0.855	0.031	4.8	5.6
16.2	351	1.04	0.039	4.2	5.4
18.5	367	1.01	0.037	4.5	6.1
25.3	403	0.984	0.037	5.0	8.6
94.0	307	1.70[c]	0.117	1.5[e]	1.5
98.0	314	1.72	0.119	1.6	2.0
103	325	1.73	0.125	1.6	2.8
110	335	1.77	0.130	1.5	2.6
113	346	1.77	0.118	1.5	3.8
120	361	1.77	0.107	1.5	4.9

[a] 1 cP = 10^{-3} Pa s.
[b] Reference 77.
[c] Extrapolated from Ref. 77 following Ref. 70.
[d] Reference 78.
[e] Extrapolated from Ref. 72.

TABLE II. Rate coefficients k for photoisomerization of *trans*-stilbene in liquid ethane, propane, and *n*-butane.

p/MPa	T/K	$[M]/10^{-2}$ mol cm^{-3}	η/cP[a]	$D/10^{-4}$ cm^2 s^{-1}	$k/10^{10}$ s^{-1}
Ethane					
6.5	295	1.22[b]	0.048[b]	3.3[g]	2.8
7.0	295	1.24	0.050	3.1	2.5
4.5	298	1.087	0.038	3.7	3.1
6.8	298	1.18	0.045	3.5	2.8
14.0	298	1.32	0.060	2.8	2.6
54.0	298	1.60	0.095	1.7	2.1
81.0	298	1.70	0.115	1.5	1.9
120	298	1.81[c]	0.159[d]	1.4	2.0
130	298	1.83	0.174	1.3	1.8
190	298	1.94	0.232	1.1	1.7
240	298	2.01	0.28	0.90	1.4
300	298	2.07	0.33	0.76	1.4
340	298	2.11	0.37	0.70	1.2
400	298	2.15	0.42	0.62	1.0
600	298	2.28	0.59	0.44	0.81
7.6	303	1.13[b]	0.045[b]	3.6	2.7
92.0	303	1.72	0.123	1.5	2.0
Propane					
0.9	298	1.12[b]	0.095[b]	1.25[h]	2.4
1.1	298	1.13	0.098	1.23	2.5
50.0	298	1.28	0.167	0.84	2.2
100	298	1.37	0.22[f]	0.68	1.5
110	298	1.38	0.23	0.65	1.5
300	298	1.55[e]	0.54	0.31	0.88
400	298	1.61	0.70	0.27	0.86
470	298	1.65	0.82	0.25	0.73
n-Butane					
5.3	298	0.996[b]	0.168[b]	0.64[i]	2.5
51.5	298	1.08	0.253[f]	0.50	1.7
150	298	1.22[c]	0.36	0.33	1.5
330	298	1.28	0.88	0.17	0.81
500	298	1.35	1.46	0.13	0.53
520	298	1.36	1.52	0.12	0.53

[a] 1 cP = 10^{-3} Pa s.
[b] Reference 77.
[c] Extrapolated from Ref. 77 following Ref. 70.
[d] Extrapolated from Ref. 80.
[e] Reference 79.
[f] Reference 80.
[g] Reference 72.
[h] Extrapolated from Ref. 81 via density dependence of ηD.
[i] Reference 82.

TABLE III. Rate coefficients k for photoisomerization of *trans*-stilbene in supercritical and liquid CO_2 and SF_6.

p/MPa	T/K	$[M]/10^{-2}$ mol cm^{-3}	η/cP^a	$D/10^{-4}$ cm^2 s^{-1}	$k/10^{10}$ s^{-1}
CO$_2$					
12.0	335	1.068^b	0.035^b	4.0^c	6.5
24.0	335	1.73	0.066	2.1^d	4.6
52.0	335	2.13	0.104	1.3	3.9
160	335	2.61	0.193	0.88	3.2
260	335	2.83	0.281	0.64	2.6
350	335	3.03	0.42	0.45	1.9
7.5	297	1.69^b	0.063^b	2.0^c	4.0
60.0	297	2.34	0.135	1.05^d	2.6
120	297	2.59	0.190	0.79	2.0
200	297	2.79	0.250	0.64	1.4
250	297	2.87	0.264	0.61	1.2
410	297	3.07	0.368	0.46	1.3
500	297	3.16	0.417	0.41	1.1
SF$_6$					
6.5	330	0.743^e	0.075^e	2.0^g	6.1
11.0	330	0.906	0.123	1.3	5.5
58.0	330	1.18^f		0.60^f	3.9
105	330	1.26		0.50	3.1
145	330	1.30		0.40	2.9
58.0	365	1.12		0.70	4.9
104	365	1.24		0.58	4.4
144	365	1.28		0.47	4.2
5.6	298	0.97^e	0.180^e	0.86^g	3.6
56.0	298	1.23^f		0.38^f	2.5
100	298	1.29		0.25	1.9
130	298	1.32		0.19	1.4
140	298	1.33		0.17	1.3

^{a} 1 cP = 10^{-3} Pa s.
^{b} Reference 83.
^{c} Reference 71.
^{d} Extrapolated from Ref. 81 via density dependence of ηD.
^{e} Reference 85.
^{f} Reference 84.
^{g} Reference 78.

TABLE IV. Rate coefficients k for photoisomerization of *trans*-stilbene in supercritical propane, xenon, and CHF_3.

p/MPa	T/K	$[M]/10^{-2}$ mol cm^{-3}	η/cP^a	$D/10^{-4}$ cm^2 s^{-1}	$k/10^{10}$ s^{-1}
Propane					
1.2	468	0.032^b	0.0128^b	233^c	5.0
22.0	384	0.995	0.070	2.0^f	5.4
56.0	384	1.15	0.106	1.3	5.2
150	384	1.34^c	0.189^d	0.90	4.0
220	384	1.41	0.256	0.70	3.9
250	384	1.44	0.28	0.68	3.1
300	384	1.48	0.32	0.59	3.2
400	384	1.55	0.43	0.47	2.9
Xenon					
9.5	298	1.29^g	0.098^h	1.67^i	4.8
22.2	298	1.57	0.147	1.17	4.1
70.0	298	1.93		0.72	3.8
100	298	2.07		0.58	3.3
160	298	2.23		0.40	3.0
CHF$_3$					
110	330	1.92^j		0.92^j	6.8
150	330	2.01		0.75	6.2
310	330	2.23		0.40	5.6

^{a} 1 cP = 10^{-3} Pa s.
^{b} Reference 77.
^{c} Reference 79.
^{d} Reference 80 extrapolated.
^{e} Reference 78.
^{f} Extrapolated from Ref. 81 via density dependence of ηD.
^{g} Reference 86.
^{h} Reference 87.
^{i} Reference 88.
^{j} Reference 89.

measured temperature coefficient of k, see below. The rate coefficients obtained in other nonpolar solvents at room temperature are plotted in Fig. 3. They appear still to be far away from the Smoluchowski limit for Xe and SF_6, whereas they approach this limit for CO_2.

In our recent work on DPB we have discussed connections between density dependent solvent shifts of the effective barriers for photoisomerization and of the UV-absorption spectra.[1] In a similar way we have now extended our earlier measurements of the pressure dependent shift of the UV-absorption maximum of *trans*-stilbene with respect to its position in the low pressure vapor at 275 nm.[31] The shifts are plotted in Fig. 4 as a function of $f(n^2) = (n^2 - 1)/(n^2 + 2)$, where n is the refractive index of the solvent. Whereas one obtains the expected linear relationship between solvent polarizability parameter and spectral shift in the regime of "normal" liquid-like densities [$f(n^2) > 0.17$], it is interesting to note the deviation from
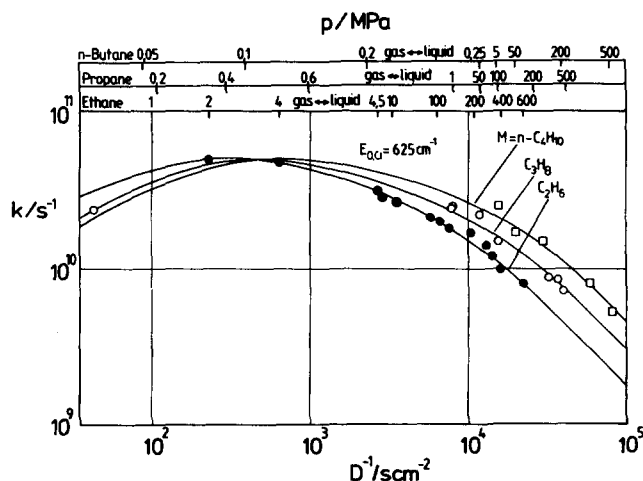

FIG. 2. Photoisomerization rate coefficients k of stilbene at $T = 298$ K in compressed ethane ($\bullet$), propane ($\bigcirc$), and *n*-butane ($\square$) vs the inverse of the self-diffusion coefficient D. The solid lines represent model fits (see Sec. 4, parameters $E_{0,\text{cl}} = 7.5$ kJ/mol and $\omega_B = 2.7 \times 10^{12}$, 4.0×10^{12}, and 6.5×10^{12} s^{-1} for ethane, propane, and *n*-butane, respectively).

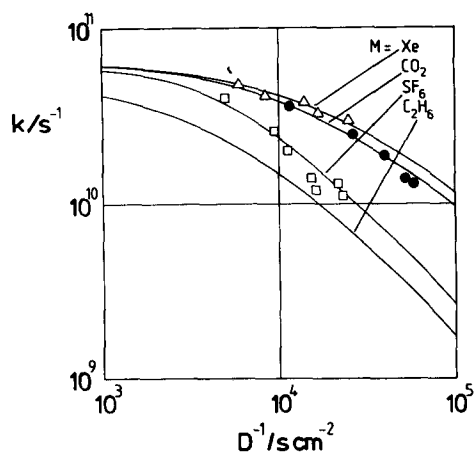FIG. 3. Photoisomerization rate coefficients k of stilbene at $T = 298$ K in CO_2 ($\square$), SF_6 ($\bullet$), and Xe ($\triangle$) vs D^{-1}. The solid lines represent model fits. (See Sec. IV, $E_{0,cl} = 6.0$ kJ/mol and $\omega_B = 2.5 \times 10^{12}$ s^{-1} for CO_2, 5.0×10^{12} s^{-1} for SF_6, and 6.0×10^{12} s^{-1} for Xe. The lowest curve, for comparison, shows the model fit for ethane from Fig. 2.)

this linear correlation towards lower densities in the gas and low pressure liquid phase in ethane, CO_2, and SF_6. This transition of the density dependence of the solvatochromic shift from gas-like to liquid-like densities has also been observed in other systems.[63]

In addition to the pressure dependence of the rate coefficient k, we also investigated its temperature dependence in supercritical ethane, propane, CO_2, and SF_6. The experiments extend earlier measurements of the temperature coefficient of k for stilbene by Courtney and Fleming in liquid ethane and propane at lower temperatures.[26] Figure 5 shows four isotherms of k vs D^{-1} in liquid and supercritical ethane, Fig. 6 shows isotherms for liquid and supercritical propane, and Fig. 7 gives the 330 K isotherms in supercritical CO_2, SF_6, and CHF_3. Whereas the rate coefficients rise with temperature, the dependence of k on D generally becomes

FIG. 5. Photoisomerization rate coefficients k of stilbene in ethane at different temperatures: 298 K ($\triangle$), 330 K ($\bullet$), 355 K ($\square$), and 375 K ($\bigcirc$). The curves represent model fits with $E_{0,cl} = 7.5$ kJ/mol, and $\omega_B(330$ K$) = 4.0 \times 10^{12}$ s^{-1}, ω_B $(355$ K$) = 5 \times 10^{12}$ s^{-1}, and $\omega_B(375$ K$) = 7.0 \times 10^{12}$ s^{-1}.

FIG. 6. Photoisomerization rate coefficients k of stilbene in propane at 298 K ($\bigcirc$) and 395 K ($\bullet$). The curves represent model fits with $E_{0,cl} = 7.5$ kJ/mol, ω_B $(298$ K$) = 4.0 \times 10^{12}$ s^{-1}, and ω_B $(385$ K$) = 7.0 \times 10^{12}$ s^{-1}.
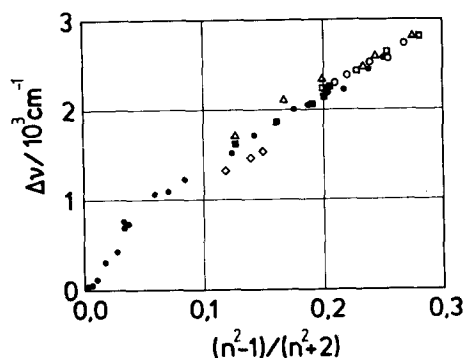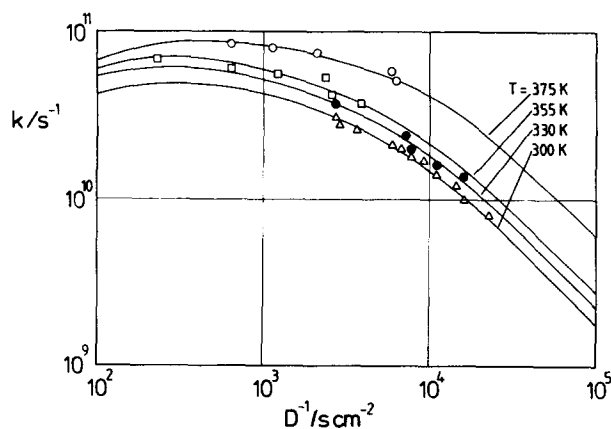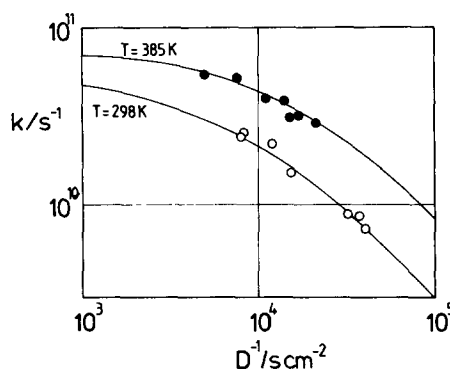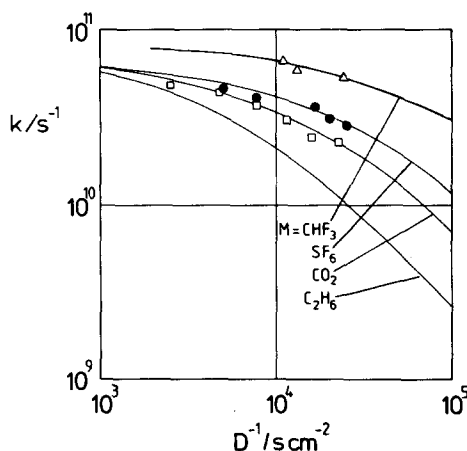

FIG. 4. Shift of the peak of the UV-absorption spectrum of trans-stilbene [in compressed ethane ($\bullet$), propane ($\bigcirc$), n-butane ($\square$), Xe ($\triangle$), CO_2 ($\blacksquare$), and SF_6 ($\diamondsuit$)] relative to the low pressure vapor spectrum as a function of the solvent polarizability parameter (n = solvent refractive index).

FIG. 7. Photoisomerization rate coefficients of stilbene at $T = 330$ K in CO_2 ($\square$), SF_6 ($\bullet$), and CHF_3 ($\triangle$). The curves represent model fits with $E_{0,cl} = 6.0$ kJ/mol and ω_B values 3.0×10^{12}, 5×10^{12}, and 1.4×10^{13} s^{-1}, respectively. The lowest curve shows the model fit for ethane at $T = 330$ K from Fig. 5.
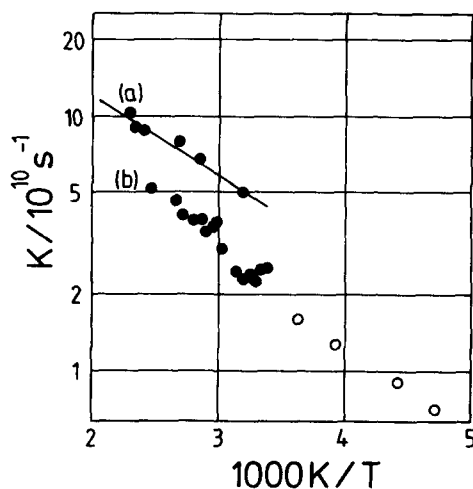
FIG. 8. Temperature dependence of the photoisomerization rate coefficient k of stilbene in ethane: (a) at low friction ($D \gtrsim 5 \times 10^{-3}$ cm^2/s) in the falloff range; (b) at high friction ($1 \times 10^{-4} < D \lesssim 5 \times 10^{-4}$ cm^2/s) in the Kramers–Smoluchowski range (in this range the measured rate coefficients have been reduced to a constant diffusion coefficient $D_0 = 3 \times 10^{-4}$ cm^2/s according to $k' = kD_0/D$; O: this work; ●: Ref. 26). The solid curve represents a model fit to the low friction data, see the text, using $E_{0,\text{cl}} = 7.5$ kJ/mol.

weaker with increasing temperature.

In order to study the temperature dependence in more detail in different density regimes, we performed a series of experiments in supercritical ethane. Figure 8 shows an Arrhenius plot of k at low densities in the falloff region of the gas phase unimolecular reaction. The figure also shows the corresponding plot for compressed liquid ethane, where the pressures were chosen in such a way that the self-diffusion coefficients were in the range $2 < D \lesssim 4 \times 10^{-4}$ cm^2 s^{-1}. In contrast to our results in DPB,[1] there appears to be no irregularity of the apparent activation energy in the vicinity of the critical temperature of ethane, $T_c = 305.4$ K. The slope of the Arrhenius plot is markedly steeper at higher than at lower densities.

IV. DISCUSSION

A. Falloff curves of the thermal unimolecular isomerization

We compare our low density results with calculations for the thermal unimolecular reaction. The high precision of the lifetime measurements in jet-cooled, isolated *trans*-stilbene molecules[4,5] allowed for the construction of an optimized RRKM fit to the specific rate coefficients $k(E,J)$ of the reaction. From this modeling the reaction threshold energy $E_0 = 15.6$ kJ/mol could be derived.[30] Thermal averaging of $k(E,J)$ over an equilibrium population $f(E,J)$ then leads to the limiting "high pressure" gas phase rate coefficient k_∞:

$$k_\infty = \int_0^\infty \int_{E_0}^\infty k(E,J)f(E,J)dE\,dJ. \tag{3}$$

As we discussed recently for the case of the photoisomerization of DPB,[1] neglecting the rotational dependence of

$k(E,J)$ leads to an uncertainty of about a factor of 2 in the value of the modeled limiting rate coefficient.[30] Including rotational effects, we obtained

$$k_\infty = 8.3 \times 10^{11} \exp(-15.0 \text{ kJ mol}^{-1}/RT) \text{ s}^{-1}$$

$$(200 \leqslant T \leqslant 450 \text{ K}). \tag{4}$$

Standard unimolecular rate theory expresses the limiting low pressure rate coefficient k_0 as[64,65]

$$k_0 = \beta_c Z_{\text{LJ}} \cdot [M] \int_0^\infty \int_{E_0}^\infty f(E,J)dE\,dJ, \tag{5}$$

where $[M]$ denotes the solvent concentration. Neglecting correction factors for rotation and anharmonicity,[64,65] i.e., $F_{\text{rot}} = I^{\neq}/I \approx 1$ and $F_{\text{anh}} \approx 1$, using a value of the collision efficiency $\beta_c \approx 1$, and estimating Lennard-Jones collision frequencies Z_{LJ}, Eq. (5) with the vibrational frequencies from Ref. 66 leads to

$$k_0 \approx 2.5 \times 10^{13} [M] \sqrt{T}$$

$$\times \exp(-2.42 \text{ kJ mol}^{-1}/RT) \text{ cm}^3 \text{ mol}^{-1} \text{ s}^{-1}. \tag{6}$$

Equations (4) and (6) govern the falloff curves for the photoisomerization under thermalized conditions. As in the case of DPB,[1] broadening effects[65] of the transition of k from k_0 to k_∞ are only of minor importance. Since we are interested only in high pressure phenomena, we also neglect the effect of incomplete thermalization after photoexcitation[67] which becomes important in low pressure thermal gases. For a representation of the $[M]$ dependence of k we, therefore, can use the simple Lindemann–Hinshelwood expression (with $k_0 \propto [M]$)

$$1/k \approx 1/k_0 + 1/k_\infty. \tag{7}$$

If one-dimensional instead of multidimensional unimolecular rate theory would apply, k_0 should be approximately $k_0 \approx 10^{14} [M] \exp(-11.5 \text{ kJ mol}^{-1}/RT) \text{cm}^3 \text{ mol}^{-1} \text{ s}^{-1}$. At a bath gas density $[M] \approx 3 \times 10^{-4}$ mol/cm^3 and $T = 468$ K, its value would be equal to $k_0 \approx 1.6 \times 10^9 \text{s}^{-1}$, which is a factor of 30 below the rate coefficient measured under these conditions (see Table IV). This "trivial" multidimensional effect is thus responsible for the high rates in the weak-damping regime.

B. Cluster effects in the low friction range

In contrast to the DPB system, where the modeled k_∞ in high pressure gases differs from the measured k only by a factor of 2,[1] in *trans*-stilbene the measured value is about one order of magnitude larger than the one derived from Eq. (3). This discrepancy is beyond the uncertainty of the analysis. The difference between the measured k and the calculated k_∞ in high pressure gases thus is clearly established. By analogy to our results for DPB,[1] we have interpreted this discrepancy in terms of specific solute–solvent interactions that can accelerate the reaction even at moderate gas pressures. The phenomenon is attributed to a solvent shift of the reaction threshold energy E_0 caused by cluster formation between *trans*-stilbene and solvent molecules M prior to excitation.[31]

The height of the reaction threshold energy in stilbene–ethane clusters can be deduced from the temperature de-

pendence of the measured rate coefficient in the low density falloff regime, see Fig. 8. At the corresponding densities ($[M] \approx 10^{-3}$ mol/cm^3), the influence of friction on the reaction rate is still negligible, and the rate coefficient is adequately represented by Eq. (7). Therefore, leaving the activated complex frequencies unchanged, we adjusted E_0 in Eqs. (3) and (5), until Eq. (7) reproduced the experimentally obtained temperature coefficient. This implies that there is essentially "complete solvation" of stilbene molecules in ethane clusters at these densities. The solid line in Fig. 8 represents the calculated temperature dependence for an energy barrier of $E_{0,cl} = 7.5$ kJ/mol.

In order to test the present cluster hypothesis, we also analyzed the stilbene photoisomerization rate coefficients measured by Balk and Fleming in gaseous methane.[33] For that purpose we describe the increasing solvation of stilbene in methane clusters by a Langmuir type "adsorption" equilibrium according to

$$\Theta([M]) = \frac{K_{cl} \cdot [M]}{(1 + K_{cl} \cdot [M])}, \qquad (8)$$

where $\Theta([M])$ varies between "0" (no solvation) and "1" (complete solvation), and K_{cl} is the equilibrium constant for the "adsorption" of methane on stilbene. Extending our simplified cluster model[31] (assuming only 1–1–solute–solvent complexes), we propose that the barrier height in the stilbene–methane cluster depends linearly on $\Theta([M])$, the fraction of coverage,

$$E_0([M]) = E_{0,free} - \Theta([M])(E_{0,free} - E_{0,cl}). \qquad (9)$$

Using Eqs. (3), (5), and (7)–(9), we fitted a barrier height $E_{0,cl} = 8.1$ kJ/mol and a value for the cluster equilibrium constant of $K_{cl} = 2.5$ dm^3/mol. The result of the fit is shown in Fig. 9 together with the falloff curves for the two limiting cases $\Theta = 0$ (only free stilbene molecules) and $\Theta = 1$ (fully clustered stilbene). The agreement between the measured points and the fitted expression from Eqs. (8) and (9) appears very satisfactory, supporting the present hypothesis.

The present model implies that, throughout the density range studied, the experimental decay curves should consist of single exponential decays, which is in agreement with the fluorescence decay measurements[32,33] and our own transient absorption experiments. This means that—at a given density—the barrier height distribution is sufficiently narrow, such that additional decay components arising from a distribution of cluster sizes cannot be observed experimentally.

Our solvent shift data of the absorption spectrum also support the cluster model. The density range, in which gradual solvation in clusters occurs, probably corresponds to the region of steeper slope in the plot of the spectral shift vs polarizability parameter in ethane, see Fig. 4. The densities here are even one order of magnitude smaller than in our kinetics experiments. This also confirms our estimate of the cluster equilibrium constant K_{cl} in ethane. The order of magnitude of K_{cl} also compares well with values we obtained for cluster formation in the iodine system,[68] where clusters govern the photolysis and recombination kinetics at pressures below those applied in the present work.
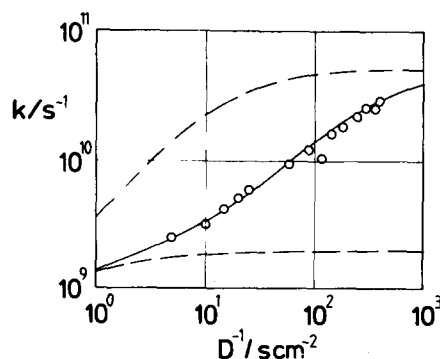

FIG. 9. Photoisomerization rate coefficient k of stilbene in methane from Ref. 33 vs D^{-1}. The lower dashed represents the falloff curve for $E_0 = 15.6$ kJ/mol, the upper dashed curve is the fall-off curve obtained for $E_{0,cl} = 8.1$ kJ/mol, both calculated according to Eqs. (3), (4), and (7). The solid line is the model fit, see the text, according to Eqs. (8) and (9) with a cluster equilibrium constant $K_{cl} = 2.5$ dm^3/mol.

The cluster hypothesis should be tested experimentally by preparing stilbene–solvent clusters in a supersonic jet. Measurements of energy specific rate coefficients $k(E)$ under such conditions should document the lowering of the reaction barrier in the cluster compared to the isolated molecule. Such experiments are underway in our laboratory. Their analysis could provide the confirmation of the $E_{0,cl}$ values derived here.

The RRKM analysis of energy specific rate coefficients $k(E)$ for the isolated molecule[30] assumes complete intramolecular vibrational energy relaxation (IVR). This assumption is in agreement with the observation that there is no evidence for mode selectivity of stilbene photoisomerization[4,5] which would indicate incomplete IVR. On the other hand, IVR has been shown to be fairly slow at small vibrational energies in the S_1 state.[8] A recent study of the deuterium isotope effect in *trans*-stilbene photoisomerization[33] also seems to be inconsistent with previous RRKM calculations[30,38] and their implications about the ordering of rate coefficients for deuterated and nondeuterated species. A theoretical model incorporating limited IVR into an RRKM-like analysis was developed[40] that qualitatively describes the experimental observations. In this model it is argued that the onset of the experimentally observed $k(E)$ in the isolated molecule is dominated by the onset of IVR and that consequently, a standard RRKM analysis does not lead to the "real" barrier height E_0 which may be lower than the value deduced from the RRKM analysis. While a model with incomplete IVR certainly provides one possibility of interpretation, at present we still favor the assumption of a reaction characterized by complete IVR. We attribute the "unexpected" isotope effects to the complicated activated complex structure such as revealed in our MNDO calculations of the potential surface for S_1 photoisomerization in stilbene.[57] Changing the normal mode pattern of the molecule by deuteration leads to changes of the projection of these modes on the lowest energy path. With complicated

activated complex structures, these effects may become almost unpredictable. These complications have not been considered in the analysis of Ref. 27, 38, and 40.

Another experimental observation appears to be relevant in relation with the discussion of IVR at energies above the threshold energy: at moderate excess energies, the decay of isolated molecules in Ref. 27 was found to be nonexponential. This observation may be explained by incomplete IVR in the isolated molecule. However, an alternative explanation may be offered by rotational effects: $k(E,J)$ very strongly depends on J.[30,34] So far none of the available experiments succeeded in the preparation of a distribution with a single J only. Therefore, the J distribution may result in nonexponential decays as well as[34] in "threshold rate constants" which are below the RRKM value of $k(E = E_0, J = 0)$.

C. Cluster effects in the high friction range

Over the whole density range, the rate coefficient can be expressed with sufficient accuracy by the connection formula[45,92]

$$1/k \approx 1/k_0 + 1/k_\infty + 1/k_{\rm diff}, \tag{11}$$

where $k_{\rm diff}$ denotes the diffusion-limited rate coefficient in the high fraction limit. In particular, numerical simulations have shown[93] that the expression $1/k_\infty + 1/k_{\rm diff}$ approximates the full Kramers equation[94] for the rate coefficient from intermediate to high damping as well as the analogous expression for the BGK model[95] to within 10%–20%, provided the rate coefficient reduces to the correct Smoluchowski limit at high friction. As we will show, this condition is fulfilled in the solvents and the range of friction discussed here. Therefore, using $k_{\rm diff}$ given by

$$k_{\rm diff} \approx (\omega_B/\beta) k_\infty \tag{12}$$

with k_∞ from Eq. (10), imaginary "barrier frequency" ω_B, and friction coefficient β in Eq. (11) is equivalent to using the connection formula $1/k \approx 1/k_0 + 1/k_{\rm Kramers}$ with $k_{\rm Kramers}$ taken from Ref. 94.

In the absence of complete potential energy calculations, the *a priori* identification of the barrier frequency still remains equally difficult as that of a reactant frequency becoming the "reaction coordinate". Therefore, we have to accept the activated complex frequency scaling parameters, such as used in optimized RRKM fits of $k(E,J)$ in Ref. 30, and imaginary barrier frequencies remain fit parameters. On the other hand, the friction coefficient β for rotation of the phenyl group can be estimated by the relationship[69]

$$\beta \approx c_1 \eta \sigma_2 r^2 / I_{\rm Ph}, \tag{13}$$

where η denotes solvent viscosity, $\sigma_2 = 0.37$ nm represents the estimated Lennard-Jones radius of the phenyl group,[70] the radius of gyration is $r = 0.25$ nm, and $I_{\rm Ph}$ is the moment of inertia of the phenyl group for rotation around the double bond, $I_{\rm Ph} \approx m_2 r^2$, with $m_2 = 1.3 \times 10^{-22}$ g. The value of c_1 depends on the boundary condition. We use $c_1 = 4\pi$ for pure slip. The Stokes–Einstein relation is used to obtain β in terms of the self-diffusion coefficient of the solvent. As experimental diffusion and viscosity on ethane and also propane[71,72] show that the ratio $D n \sigma_1 / k_B T = c_2$ is not constant

with pressure, we use appropriately interpolated values for c_2.

The solid lines in Fig. 2 are the result of modeling the dependence of the rate coefficient on D^{-1} using $E_{0,\rm cl}$ and ω_B as fit parameters and assuming that $f_{\rm cl} \approx 1$ at liquid phase densities. The best fit for all three solvents was obtained with a reaction threshold of 7.5 kJ/mol, which is the same value as determined from the low friction data in ethane and methane (see Sec. IV B). In each of the solvents one observes that k approaches proportionality to D at the highest pressures applied. Changing the solvent, however, causes a shift of the turnover to diffusion control along the D^{-1} axis, whereas the slope of the curve in the high friction range does not change. This shift cannot be understood in terms of variations of solvent transport parameters such as friction coefficient, viscosity, or frequency dependent friction alone. There is also no reason to attribute these shifts to failures of the Stokes–Einstein relation, since this relation appears to be valid for each individual solvent. This behavior appears to be in contrast with earlier observations of *trans*-stilbene photoisomerization in compressed liquid hexane.[73] The deviations from the prediction of the simple Kramers–Smoluchowski expression observed here and also in other higher *n*-alkanes (larger than *n*-octane) at ambient pressure[19,25,28,42,74,75] and therefore, seem to be restricted either to a regime of viscosities higher than about 1 cP, or they represent a solvent size effect coming into play as the alkane chain length increases. In and case, they are of no significance for the measurements we discuss here.

The most plausible explanation of the observed shifts of the $k(D^{-1})$ curves along the D^{-1} axis appears to be again a cluster- or solvent-induced modification of the potential energy surface. Whereas modifications of the barrier height were considered in Sec. IV B, we now also have to suggest modifications of the imaginary barrier frequency ω_B by clustering. The curves in Fig. 2 were fitted with $\omega_B = 2.7 \times 10^{12}$, 4.0×10^{12}, and 6.5×10^{12} s^{-1} for ethane, propane, and *n*-butane, respectively. These values of ω_B are lower than the double bond torsional mode frequency, such as noted before[19,43] in connection with the observation of an anomalous viscosity dependence of the rate coefficient in a series of different solvents. The low values of ω_B indicate a very flat barrier to rotation around the double bonds, in agreement with our MNDO calculations for stilbene.[57] The concept of a reaction being governed by a single torsional mode of the molecule apparently is not sufficient here.[1,76] Our MNDO calculations showed that there is a marked dependence of the S_1 energy on the phenyl ring twist angle, and that the equilibrium configurations of ground and lowest excited state show a different angle, the molecule being more planar in the excited S_1 state. If the phenyl ring equilibrium configuration in ground and excited state is affected by the environment, such as clustering with solvent molecules, one can understand the marked influence on both the height and the shape of the barrier.

The solvent specificity of these effects is further supported by the analysis of the experimental rate coefficients in liquid CO_2, SF_6, and supercritical xenon at room temperature in the same density range. The curves in Fig. 3 represent

model calculations using $E_{0,cl} = 6.0$ kJ/mol for all three solvents together with ω_B values of 2.5×10^{12} s^{-1} for CO_2, 5.0×10^{12} s^{-1} for SF_6, and 6.0×10^{12} s^{-1} for Xe. Especially the parameter ω_B seems to be very susceptible to changes of solvent. (One should note that the fit of $E_{0,cl}$ is not completely independent of the ω_B values chosen.) In summarizing this section we conclude that there is ample evidence for solvent specific clustering which modifies the shape of the potential in the activated complex range (barrier height and imaginary barrier frequency) for the S_1 photoisomerization of *trans*-stilbene.

D. Multidimensional barrier effects in the Kramers–Smoluchowski range

Fitting barrier height and imaginary barrier frequency for individual solvents allows for a satisfactory representation of all pressure-dependent rate coefficients k at constant temperature. We now investigate whether the temperature dependence of k can be represented in this way as well. We consider the high friction limiting Kramers–Smoluchowski range. Inspection of Figs. 5, 6, and 8 indicates that the temperature dependence in this range is stronger than in the low friction transition range to k_∞. Like in the case of DPB photoisomerization,[1] the effect markedly exceeds that of the temperature dependence of the friction. We think that this effect—as in DPB—is best accommodated by introducing a temperature dependence of the "apparent barrier frequency ω_B" of the one-dimensional Kramers expression which accounts for the multidimensionality of the potential energy surface. The solid curves in Fig. 5 were obtained by keeping $E_{0,cl} = 7.5$ kJ/mol fixed and using fitted apparent barrier frequencies $\omega_B = 2.7 \times 10^{12}$ s^{-1} at 298 K, $\omega_B = 5.0 \times 10^{12}$ s^{-1} at 355 K, and $\omega_B = 7.0 \times 10^{12}$ s^{-1} at $T = 375$ K. The curves in Fig. 6 show the corresponding fits to the propane isotherms with $E_{0,cl} = 7.5$ kJ/mol, $\omega_b(298\ K) = 4.0 \times 10^{12}$ s^{-1}, and $\omega_B(385\ K = 7.0 \times 10^{12}$ s^{-1}. For the isotherms at 330 K in CO_2, SF_6, and CHF_3 (Fig. 7) with $E_{0,cl} = 6.0$ kJ/mol we fit the ω_B values 3.0×10^{12}, 5.0×10^{12}, and 1.4×10^{13} s^{-1}, respectively. The comparatively high values of ω_B in the probably strongly interacting polar solvent CHF_3 is worth noticing.

The increase of the temperature coefficient of k in the Kramers–Smoluchowski range beyond the prediction of a one-dimensional model with a temperature independent effective imaginary barrier frequency is less pronounced than in the DPB system. We illustrate this in Fig. 10, in which, for ethane, a "reduced rate coefficient" k_{red} is shown being defined by[1]

$$k_{red}(T) = k(T) \cdot [1 + \beta(T)/\omega_B(295\ K)]. \quad (14)$$

For the one-dimensional Kramers–Smoluchowski model of Eqs. (11) and (12)—neglecting the k_0 term—$k_{red}(T)$ should be equal to $k_\infty(T)$, which is also shown in Fig. 10 for comparison. The different slopes of $k_{red}(T)$ and $k_\infty(T)$ over the entire temperature range are quite evident. In our recent discussion of this effect in the DPB system[1] we have inspected barrier anharmonicity (i.e., deviation from an inverted parabola) and multidimensional barrier crossing as possible explanations for this behavior. Although the
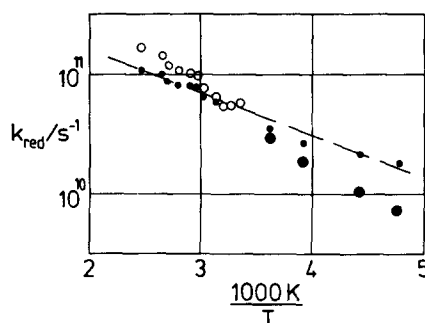

FIG. 10. Temperature dependence of the reduced rate coefficient k_{red} of Eq. (14): (O) this work; (●) Ref. 26. Dashed line: k_∞ with $E_{0,cl} = 7.5$ kJ/mol. The small points (·) are the reduced rate coefficients obtained by assuming an effective temperature dependence of the "apparent barrier frequency" ω_B (see the text).

corresponding temperature effect in stilbene seems to be somewhat less pronounced than in DPB, anharmonicity effects are still by far too small to account for the larger temperature coefficient of $k_{red}(T)$.

Our MNDO calculations for stilbene[57] suggest that the barrier "sharpens," when at least one coordinate "perpendicular" to the reaction coordinate is excited. One such coordinate was identified to be the orientation of the phenyl rings relative to the plane of the ethylene bridge. In order to demonstrate which type of potential energy surface we have in mind, in Fig. 11 we have sketched the saddle point area. The reaction coordinate is denoted by q_1, one mode perpendicular to the reaction coordinate is denoted by q_2. We represent[1] an increase of the imaginary barrier frequency ω_B of the reaction coordinate q_1 with excitation of at least one other coordinate, e.g., the coordinate q_2, in the form

$$\omega_B(E_2) \approx \omega_{B0} \cdot (E_2/a)^b, \quad (15)$$

where ω_{B0} is the imaginary barrier frequency at the saddle point, i.e., at an excitation energy $E_2 = 0$ of the coordinate
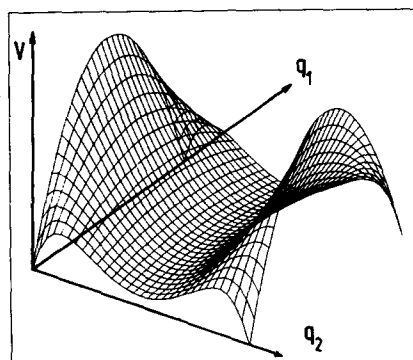

FIG. 11. Schematic representation of a potential energy surface $V(q_1, q_2)$ which shows a "sharpening" of the imaginary barrier frequency ω_B of the reaction coordinate q_1, when a perpendicular coordinate q_2 is excited (see the text). For the surface shown here, ω_B varies according to Eq. (15) with $b = 4$.

q_2. The parameters a and b describe the dependence of ω_B on the excitation energy E_2. Implementing Eq. (15) into a multidimensional Kramers–Smoluchowski treatment[1] leads to an "apparent barrier frequency $\omega_B(T)$" in the one-dimensional Kramers–Smoluchowski expression of Eq. (12) of

$$\omega_B(T) \approx \omega_{B0} \cdot (k_B T/a)^b \cdot \Gamma(b+1) \qquad (16)$$

which can be strongly temperature dependent. (A multidimensional treatment of the full Kramers expression including the intermediate damping regime would have been considerably more complicated and not reasonable at this stage.)

In the present case, a value of $b \approx 3.9$ brings the temperature dependence of the reduced rate coefficient $k_{red}(T)$ in approximate agreement with the predicted $k_\infty(T)$, as indicated by the small points in Fig. 10. The corresponding value for DPB in ethane was 4.9. As stated before,[1] $b = \Sigma_i b_i$ may include the contributions from several coordinates i "perpendicular" to the reaction coordinate. Barrier anharmonicity would have contributed to a temperature dependence of $\omega_B(T)$ with $b = 0.5$ at most.

In comparing our treatment with the two-dimensional model for barrier crossing proposed by Agmon and Kosloff,[54] we note that the two approaches treat the problem in different ways. Agmon and Kosloff suggest that the motion is viscosity dependent in only one coordinate. They also assume a reaction surface where the barrier height in the reaction coordinate depends on the perpendicular coordinate, i.e., the phenyl twist angle. Their treatment in effect leads to a viscosity dependent barrier height that could provide an explanation for the non-Kramers viscosity dependence of the rate coefficient in the high friction regime. Recently, Park and Waldeck[90] have adopted this model in the intermediate friction regime to interpret their extensive measurements of the S_1 photoisomerization of substituted stilbene in linear alkane solvents at ambient pressure. They stress the inadequacy of the one-dimensional Kramers model and the importance of including the phenyl ring motion. While we agree with this conclusion, we have some reservations concerning the way it was derived from isoviscosity plots in different solvents, disregarding a possible solvent dependence of the potential energy surface. Considering the surprisingly high temperature coefficient at fixed viscosity in the intermediate friction regime, our analysis shows that variations in the barrier curvature (imaginary barrier frequency) with both solvent and thermal excitation of the perpendicular coordinate seem to play the more important role. We also note that the kind of surface employed in Ref. 54 at most can lead to a linear dependence of ω_B on temperature.

Neglecting these differences in emphasis and argument it seems clear, however, that experiments under a variety of conditions probe different details of the potential energy surface, which itself, of course, has to be viscosity and temperature independent. The experiments clearly begin to reveal the multidimensional character of the surface. Whether the surface itself is modified by solute–solvent interactions or whether one is probing different reaction paths on the same surface in different solvents remains to be clarified. In any case, a simple one-dimensional picture is not sufficient. In

view of the experimental information available, attempts to save concepts such as the one-dimensional Kramers model or the constant intrinsic reaction barrier[41] appear to lead to an inadequate parametrization of the potential energy surface. Representing[41] observed activation enthalpies in n-alkanes (C_5–C_{16}) as the sum of an intrinsic barrier for twisting, which is independent of solvent, and the activation energy for viscous flow in the solvent, neglects many of the experimental observations we have discussed in detail above. For the smaller alkanes, we did not find pressure dependent intrinsic barriers, which represent one of the effects behind formal "activation volumes." This does not mean that such effects are not present in higher alkane solvents. A complete separation of the observed effects in terms of frequency dependent friction, pressure dependent barrier shifts, multidimensional barrier crossing, etc. is a difficult task. It cannot be accomplished by the analysis[41,91] of measurements at ambient pressure alone. Additional studies of the temperature and pressure dependence appear obligatory.

V. CONCLUSIONS

In the present article we have presented evidence for solvent-cluster induced modifications of the potential energy surface of the photoisomerization of trans-stilbene. Our analysis allowed us to deduce the threshold energy for isomerization in stilbene–solvent clusters with ethane and methane. In addition to this, the multidimensionality of the potential energy surface manifests itself experimentally. Our experiments suggest that such effects can be identified via the temperature dependence of the rate coefficients in the Kramers–Smoluchowski range. At constant temperature, the Kramers–Smoluchowski representation works well for the low viscosity solvents considered in the present work. In order to clarify the mechanisms responsible for the lowering of the reaction threshold energy at high densities compared to the value determined under collision-free conditions, detailed quantum-chemical calculations of the potential energy surface of the free and the clustered molecule appear indispensable. In addition, photoisomerization experiments with isolated stilbene–solvent clusters are necessary.

[1] Ch. Gehrke, J. Schroeder, D. Schwarzer, J. Troe, and F. Voß, J. Chem. Phys. 92, 4805 (1990).
[2] J. Saltiel and J. L. Charlton, in Rearrangements in Ground and Excited States, edited by P. de Mayo (Academic, New York, 1980) Vol. 3, p. 25; J. Saltiel, J. D'Agostino, E. D. Megarity, L. Metts, K. R. Neuberger, M. Wrighton, and O. C. Zafiriou, Org. Photochem. 3, 1 (1973).
[3] R. M. Hochstrasser, Int. J. Pure Appl. Chem. 52, 2683 (1980).
[4] J. A. Syage, W. R. Lambert, P. M. Felker, A. H. Zewail, and R. M. Hochstrasser, Chem. Phys. Lett. 88, 268 (1982); J. A. Syage, P. M. Felker, and A. H. Zewail, J. Chem. Phys. 81, 4685, 4706 (1984).
[5] A. Amirav and J. Jortner, Chem. Phys. Lett. 95, 295 (1983); T. J. Majors, U. Even, and J. Jortner, J. Chem. Phys. 81, 2330 (1984).

[6] P. M. Felker and A. H. Zewail, J. Phys. Chem. **89**, 5402 (1985).

[7] N. F. Scherer, J. F. Shepanski, and A. H. Zewail, J. Chem. Phys. **81**, 2181 (1984); N. F. Scherer, J. W. Perry, F. E. Doany, and A. H. Zewail, J. Phys. Chem. **89**, 894 (1985).

[8] P. M. Felker, W. M. Lambert, and A. H. Zewail, J. Chem. Phys. **82**, 3003 (1985).

[9] N. F. Scherer, L. R. Khundkar, T. S. Rose, and A. H. Zewail, J. Phys. Chem. **91**, 6478 (1987).

[10] B. I. Greene, R. M. Hochstrasser, and R. B. Weisman, J. Chem. Phys. **71**, 544 (1979); Chem. Phys. **48**, 289 (1980).

[11] B. I. Greene and R. C. Farrow, J. Chem. Phys. **78**, 3336 (1983).

[12] J. W. Perry, N. F. Scherer, and A. H. Zewail, Chem. Phys. Lett. **103**, 1 (1983).

[13] D. K. Negus, D. S. Green, and R. M. Hochstrasser, Chem. Phys. Lett. **117**, 409 (1985).

[14] A. J. Bain, P. J. McCarthy, and R. M. Hochstrasser, Chem. Phys. Lett. **125**, 307 (1986).

[15] A. B. Myers, P. L.Holt, M. A. Pereira, and R. M. Hochstrasser, Chem. Phys. Lett. **130**, 265 (1986).

[16] O. Teschke, E. P. Ippen, and G. Holtom, Chem. Phys. Lett. **52**, 233 (1977).

[17] F. Heisel, J. A. Miehe, and B. Sipp, Chem. Phys. Lett. **61**, 115 (1979).

[18] B. I. Greene, R. M. Hochstrasser, and R. B. Weisman, Chem. Phys. Lett. **62**, 427 (1979).

[19] G. Rothenberger, D. K. Negus, and R. M. Hochstrasser, J. Chem. Phys. **79**, 5360 (1983).

[20] V. Sundström and T. Gillbro, Chem. Phys. Lett. **109**, 538 (1984).

[21] E. Akesson, H. Bergström, V. Sundström, and T. Gillbro, Chem. Phys. Lett. **126**, 385 (1986).

[22] M. Sumitani, N. Nakashima, K. Yoshihara, and S. Nagakura, Chem. Phys. Lett. **51**, 183 (1977).

[23] J. R. Taylor, M. C. Adams, and W. Sibbett, Appl. Phys. Lett. **35**, 590 (1979).

[24] H. P. Good, U. P. Wild, E. Haas, E. Fischer, E.-P. Resewitz, and E. Lippert, Ber. Bunsenges. Phys. Chem. **86**, 126 (1982).

[25] V. Sundström and T. Gillbro, Ber. Bunsenges, Phys. Chem. **89**, 222 (1985).

[26] S. F. Courtney and G. Fleming, J. Chem. Phys. **83**, 215 (1985).

[27] S. H. Courtney, M. W. Balk, L. A. Phillips, S. P. Webb, D. Yang, D. H. Levy, and G. R. Fleming, J. Chem. Phys. **89**, 6697 (1988).

[28] S. K. Kim and G. R. Fleming, J. Phys. Chem. **92**, 2168 (1988).

[29] S. K. Kim, S. H. Courtney, and G. R. Fleming, Chem. Phys. Lett. **159**, 543 (1989).

[30] J. Troe, Chem. Phys. Lett. **114**, 241 (1985).

[31] J. Schroeder and J. Troe, Chem. Phys. Lett. **116**, 453 (1985); G. Maneke, J. Schroeder, J. Troe, and F. Voβ, Ber. Bunsenges. Phys. Chem. **89**, 896 (1985).

[32] M. Lee, G. R. Holtom, and R. M. Hochstrasser, Chem. Phys. Lett. **118**, 359 (1985).

[33] M. W. Balk and G. R. Fleming, J. Phys. Chem. **90**, 3975 (1986).

[34] J. Troe, A. Amirav, and J. Jortner, Chem. Phys. Lett. **115**, 245 (1985).

[35] G. Maneke, J. Schroeder, J. Troe, and F. Voβ, in *Time Resolved Vibrational Spectroscopy*, edited by A. Laubereau and M. Stockburger (Springer, Berlin, 1985), Vol. 4, p. 156.

[36] J. Schroeder and J. Troe, Annu. Rev. Phys. Chem. **38**, 163 (1987).

[37] J. Schroeder and J. Troe, J. Phys. Chem. **90**, 4215 (1986); J. Troe, *ibid.* **90**, 357 (1986).

[38] L. R. Khundkar, R. A. Marcus, and A. H. Zewail, J. Phys. Chem. **87**, 2473 (1983).

[39] P. M. Felker and A. H. Zewail, J. Phys. Chem. **89**, 5402 (1985).

[40] S. Nordholm, Chem. Phys. **137**, 109 (1989).

[41] J. Saltiel and Y.-P. Sun, J. Phys. Chem. **93**, 6246 (1989); Y.-P. Sun and J. Saltiel, *ibid.* **93**, 8310 (1989).

[42] G. R. Fleming, S. H. Courtney, and M. W. Balk, J. Stat. Phys. **42**, 83 (1986).

[43] S. P. Velsko and G. R. Fleming, J. Chem. Phys. **76**, 3553 (1982).

[44] J. Troe, Habilitationsschrift, Göttingen, 1967.

[45] J. Troe, in *High Pressure Chemistry*, edited by H. Kelm (Reidel, Dordrecht, 1978), p. 489.

[46] J. Troe, in *Physical Chemistry. An Advanced Treatise*, edited by W. Jost (Academic, New York, 1975), Vol. VIB, p. 835.

[47] For recent reviews see: J. T. Hynes, in *The Theory of Chemical Reaction Dynamics*, edited by M. Baer (Chemical Rubber, Boca Raton, 1985), Vol. 4, p. 171; J. T. Hynes, Annu. Rev. Phys. Chem. **36**, 573 (1985); J. Stat. Phys. **42**, 149 (1986); G. H. Weiss, *ibid.* **42**, 3 (1986); P. Hänggi,

ibid. **42**, 105 (1986); F. Marchesoni, Adv. Chem. Phys. **63**, 603 (1986); D. Chandler, J. Stat. Phys. **42**, 49 (1986); J. A. Montgomery, Jr., D. Chandler, and B. J. Berne, J. Chem. Phys. **70**, 4056 (1979); J. E. Straub, M. Borkovec, and B. J. Berne, *ibid.* **84**, 1788 (1986); J. E. Straub and B. J. Berne, *ibid.* **85**, 2999 (1986); R. E. Cline, Jr. and P. G. Wolynes, *ibid.* **86**, 3836 (1987); R. O. Rosenberg, B. J. Berne, and D. Chandler, Chem. Phys. Lett. **75**, 162 (1980); D. Statman and G. W. Robinson, J. Chem. Phys. **83**, 655 (1985); A. Nitzan, *ibid.* **86**, 2734 (1987); J. E. Straub and B. J. Berne, *ibid.* **87**, 6111 (1987); M. Borkovec and B. J. Berne, *ibid.* **82**, 794 (1985); A. Nitzan, *ibid.* **82**, 1614 (1985).

[48] R. Landauer and J. A. Swanson, Phys. Rev. **121**, 1668 (1961).

[49] J. S. Langer, Ann. Phys. **54**, 258 (1969).

[49] Z. Schuss and B. J. Matkowsky, SIAM J. Appl. Math. **35**, 604 (1979).

[50] H. Weidenmüller and Z. Jing-Shang, J. Stat. Phys. **34**, 191 (1984).

[51] M. M. Klosek-Dygas, B. M. Hoffmann, B. J. Matkowsky, A. Nitzan, M. A. Ratner, and Z. Schuss, J. Chem. Phys. **90**, 1141 (1989).

[52] A. M. Berezhkovskii, L. M. Berezhkovskii, and V. Yu. Zitzerman, Chem. Phys. **130**, 55 (1989); A. M. Berezhkovskii and V. Yu. Zitzerman, Chem. Phys. Lett. **158**, 369 (1989).

[53] S. Lee and M. Karplus, J. Phys. Chem. **92**, 1075 (1988).

[54] N. Agmon and R. Kosloff, J. Phys. Chem. **91**, 1988 (1987).

[55] B. J. Matkowsky, A. Nitzan, and Z. Schuss, J. Chem. Phys. **88**, 4765 (1988); **90**, 1292 (1989).

[56] R. S. Larson and M. D. Kostin, J. Chem. Phys. **77**, 5017 (1982).

[57] J. Troe and K.-M. Weitzel, J. Chem. Phys. **88**, 7030 (1988).

[58] H. E. Lessing and A. von Jena, Chem. Phys. Lett. **42**, 213 (1976).

[59] K. Yoshihara, A. Namiki, M. Sumitani, and N. Nakashima, J. Chem. Phys. **71**, 2892 (1979).

[60] S. Sharafy and K. A. Muszkat, J. Am. Chem. Soc. **93**, 4119 (1971).

[61] F. E. Doany, R. M. Hochstrasser, B. I. Greene, and R. R. Millard, Chem. Phys. Lett. **118**, 1 (1985).

[62] B. I. Lee and M. G. Kesler, A. I. Chem. Eng. J. **21**, 510 (1975); J. O. Hirschfelder, C. F. Curtiss, and R. B. Bird, *Molecular Theory of Gases and Liquids* (Wiley, New York, 1954).

[63] S. L. Frye, C. R. Yonker, D. R. Kalkwarf, and R. D. Smith, in *Supercritical Fluids*, edited by T. G. Squires and M. E. Paulaitis, ACS Symp. Ser. (American Chemical Society, Washington, D. C., 1987), **329**, p. 27.

[64] J. Troe, J. Chem. Phys. **66**, 4745, 4758 (1977).

[65] J. Troe, J. Phys. Chem. **83**, 114 (1979).

[66] A. Warshel, J. Chem. Phys. **62**, 214 (1975).

[67] J. Troe, J. Phys. Chem. **87**, 1800 (1983).

[68] B. Otto, J. Schroeder, and J. Troe, J. Chem. Phys. **81**, 202 (1984); H. Hippler, K. Luther, and J. Troe, Ber. Bunsenges. Phys. Chem. **77**, 1104 (1973).

[69] J. S. McCaskill and R. G. Gilbert, Chem. Phys. **44**, 389 (1979).

[70] R. C. Reid, J. M. Prausnitz, and T. K. Sherwood, *The Properties of Gases and Liquids* (McGraw-Hill, New York, 1977).

[71] R. C. Robinson and W. E. Stewart, I&EC Fundam. 7, 91 (1968); P.M. Holland, H. J. M. Hanley, K. E. Gubbins, and J. M. Haile, J. Phys. Chem. Ref. Data **8**, 559 (1979); H. J. M. Hanley, K. E. Gubbins, and S. Murad, *ibid.* **6**, 1167 (1977); **10**, 799 (1981).

[72] C. G. Wade and J. S. Waugh, J. Chem. Phys. **43**, 3555 (1965).

[73] L. A. Brey, G. B. Schuster, and H. G. Drickamer, J. Am. Chem. Soc. **101**, 129 (1979).

[74] S. H. Courtney, S. K. Kim, S. Canonica, and G. R. Fleming, J. Chem. Soc. Faraday Trans. 2 **82**, 2065 (1986).

[75] M. Lee, A. J. Bain, P. J. McCarthy, C. H. Han, J. N. Haseltine, A. B. Smith III, and R. M. Hochstrasser, J. Chem. Phys. **85**, 4341 (1986).

[76] E. Pollak, J. Chem. Phys. **86**, 3944 (1987).

[77] B. A. Younglove and J. F. Ely, J. Phys. Chem. Ref. Data **16**, 577 (1987).

[78] A. Boushehri, J. Bziwski, J. Kestin, and E. A. Mason, J. Phys. Chem. Ref. Data **16**, 445 (1987).

[79] S. E. Babb, Jr. and S. L. Robertson, J. Chem. Phys. **53**, 1097 (1970).

[80] S. E. Babb, Jr. and G. J. Scott, J. Chem. Phys. **40**, 3666 (1964).

[81] J. H. Dymond, Chem. Phys. **17**, 101 (1976).

[82] F. Bachl and H.-D. Lüdemann, Z. Naturforsch. Teil A **41**, 963 (1986).

[83] A. Michels, A. Botzen, and W. Schuurman, Physica **23**, 95 (1957); W. Kurin and I. F. Golubev, Teploenergetika **21**, 84 (1974).

[84] J. DeZwaan and J. Jonas, J. Chem. Phys. **63**, 4606 (1975).

[85] J. H. B. Hoogland, H. R. van den Berg, and N. J. Trappeniers, Physica A **134**, 169 (1985).

[86] A. Michels, T. Wassenaar, G. J. Wolkers, and J. Dawson, Physica **22**, 17 (1956); D. Vidal, L. Guengant, and J. Vermesse, Physica A **116**, 227 (1982).

[87] H. J. M. Hanley, R. D. McCarty, and W. M. Hynes, J. Phys. Chem. Ref.

Data **3**, 979 (1974).

[18] P. W. E. Peereboom, H. Luigjes, and K. O. Prins, Physica A **156**, 260 (1989).

[19] E. W. Lang, F. X. Prielmeier, H. Radkowitsch, and H.-D. Lüdemann, Ber. Bunsenges. Phys. Chem. **91**, 1025 (1987).

[20] N. S. Park and D. H. Waldeck, J. Chem. Phys. **91**, 943 (1989).

[91] The criticism (Ref. 41) of earlier identifications of apparent activation energies of k_{TST} with the threshold energy E_0 is incorrect. Representing k_{TST} by $k_{TST} = (kT/h)Q^{\neq}/Q \exp(-E_0/kT)$ and assuming that the reaction coordinate corresponds to a low frequency mode ($/hc \approx 10^2$ cm^{-1}) leads to $k_{TST} \approx \exp(-E_0/kT)$ if the contributions of all other modes cancel. The value of the intrinsic activation enthalpy given in Ref. 41 then corresponds to $E_0 - RT$, and not to E_0 as claimed.

[92] B. J. Berne, M. Borkovec, and J. E. Straub, J. Phys. Chem. **92**, 3711 (1988).

[93] M. Borkovec, Ph.D. Thesis, Columbia University, 1986.

[94] H. A. Kramers, Physica **7**, 284 (1940).

[95] J. T. Hynes, Chem. Phys. Lett. **79**, 344 (1981).